Electronic Effects on the Ground-State Rotational Barrier of Polyene Schiff Bases: A Molecular Orbital Study

Béla Paizs,† Emadeddin Tajkhorshid, and Sándor Suhai*

Department of Molecular Biophysics, German Cancer Research Center, Im Neuenheimer Feld 280, D-69120 Heidelberg, Germany

Received: June 15, 1998; In Final Form: April 15, 1999

The energetics of a double bond rotation in neutral and protonated polyene Schiff bases is investigated by means of quantum chemical methods. In the case of small neutral and protonated imines the performance of various quantum chemical methods including closed-shell and open-shell Hartree−Fock (HF), closed-shell and open-shell density functional theory (DFT), complete active space self-consistent field (CAS-SCF), and unrestricted natural orbital complete active space (UNO-CAS) is compared to one another. The efficiency of these methods is carefully investigated, and in the protonated case comparison of theoretical and experimental vibrational spectra is also used for the verification of the methods. These evaluations show that the rotation of the double bond neighboring the imine group can be well described at the B3LYP/6-31G(d) or UB3LYP/6-31G(d) levels in the case of protonated or neutral Schiff bases, respectively. The calculated rotational barriers in the case of the protonated and neutral *N*-methylretinal Schiff base are 23.5 and 35.7 kcal/mol, respectively. The results are interpreted by various mesomeric structures of the trans and rotated species.

Introduction

Retinal proteins[1−11] are widely used by living organisms for such different purposes as light detection and energy transport. Despite the differences concerning the details of the molecular mechanism of their function, retinal proteins use basically the same chromophore and light reaction. Both light detection and energy transfer are started by absorption of a photon, and then the chromophore is isomerized in the excited state. Afterward, the reaction proceeds along several intermediates, and finally, the photoreaction cycles back.

One of the most widely studied retinal proteins is bacteriorhodopsin (BR) present in the outer purple membrane of *Halobacterium salinarium* (formerly *H. halobium*). BR is one of the simplest known active membrane transport systems. It functions as a light-driven proton pump converting light energy into a proton gradient that is used by the cell as an energy source to activate ATP synthase. Structurally, it folds into seven transmembrane helices, one of them containing the residue Lys_{216} at which the retinal prosthetic group binds via a protonated Schiff base linkage (for reviews see refs 1−11).

Thermally activated rotation around a double bond in the retinal Schiff base (Figure 1) has been demonstrated in the so-called dark adaptation process of BR. Dark adaptation involves a reversible thermally activated transition between the two spectroscopically different forms of the pigment, BR_{568} and BR_{548}, which, at room temperature, occurs with a half-time of about 1 h. The retinal isomer composition in BR is 66% 13 cis and 34% all trans in the dark adapted form of the pigment, a ratio that is altered in mutants of BR and in bacterial rhodopsins of other species.[12]

Dark adaptation is believed to proceed through either isomerization around the 13−14 double bond or co-isomerization around 13−14 and 15−N retinal double bonds (bicycle pedal motion[13]). In a recent paper Logunov and Schulten published their combined quantum chemistry and molecular dynamics (MD) study[14] of the "bicycle pedal" model. These authors carried out MD calculations based on classical force fields and used quantum chemical methods for describing the chromophore at selected geometries. In the quantum chemical calculations the electrostatic effect of the protein environment was considered through explicit point charges in the electronic Hamiltonian. Logunov and Schulten found that the placement of retinal into BR reduced the calculated isomerization barrier and that the protein environment had a substantial electronic and steric effect on this process.

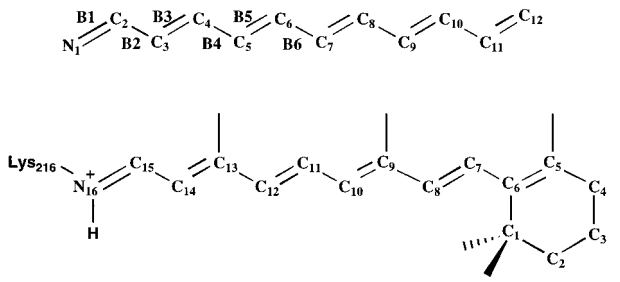

Figure 1. Atom and bond numbering used in the text in the case of the all trans structure of the Schiff base with six conjugated double bonds (SB6) (top). Retinal Schiff base structure in the ground state of the BR photocycle and its conventional numbering scheme (bottom).

In the present study, we investigate the effect of internal structural properties of polyene Schiff bases on the torsional barrier to the rotation around the neighboring double bond of the imine group (Figure 1). Different aspects of the conjugated Schiff base structures, including the length of the conjugated polyene chain, different protonation states, and the effect of methyl substituents on the main chain are studied applying different ab initio methodological approaches. One of the most important questions concerning the theoretical modeling of a

* To whom all correspondence should be addressed. Fax: +49 6221 422333. Phone: +49 6221 422369. E-mail: S.Suhai@DKFZ-Heidelberg.de.
† Permanent address: Central Research Institute for Chemistry of the Hungarian Academy of Sciences, P.O. Box 17, 1525 Budapest, Hungary.

10.1021/jp982624l CCC: $18.00
Published on Web 06/06/1999

rotation around a double bond is what kind of quantum chemical methods should be used for the description of the system. The rotation around a perfect double bond represents a particular case of bond dissociation, and because of the biradical character (strong nondynamical correlation) of the transition state, it cannot be treated by one-determinant-based methods such as closed-shell restricted Hartree−Fock (RHF) or density functional theory (DFT) methods. Furthermore, the description of the polyene wave functions usually suffers from the presence of low-lying excited states (moderate nondynamical correlation effects), a problem that cannot be treated by one-determinant wave functions either. In those cases when strong or moderate nondynamical correlation effects cause difficulties, one has to use open-shell or multideterminant wave functions. These cases are usually accompanied by the appearance of triplet instability of the underlying RHF model. This means that one can find a singlet unrestricted Hartree−Fock (UHF) solution with a total energy that is lower than the corresponding RHF value. In this case one can either use the UHF (or unrestricted DFT) methods or can change for a real multideterminantal description like the complete active space self-consistent field[15] (CAS-SCF) and unrestricted natural orbital complete active space[16] (UNO-CAS) methods. One has to mention here that the unrestricted methods suffer from some deficiencies. It is rather often that the closed-shell solution is triplet-stable in some parts of the investigated potential energy surface (PES). Furthermore, the spin contamination of the simple unrestricted models varies from point to point on the PES, making the description of the PES unbalanced.

Comparison of CAS-SCF (UNO-CAS) and DFT (open-shell DFT) results can help us to clarify whether the DFT methods can describe the nondynamical correlation effects manifested in delocalized π-electron systems such as conjugated Schiff bases. It is to be noted that there are some studies reported in the literature concerning the ability of DFT to model not only dynamical but also nondynamical correlation effects. For example, Pulay and co-workers calculated the geometry and vibrational spectra of azulene[17] using DFT and UNO-CAS methods to answer the question of whether the minimum has C_{2v} or C_s symmetry. The UNO-CAS method gave one of the bond-alternating C_s structures, while DFT led to the bond-equalized one. Both the UNO-CAS and B3LYP frequencies were close to the experimental values except for the bond alternation mode, which was better described by the DFT method showing that the equilibrium geometry of azulene is bond-equalized with C_{2v} symmetry. Furthermore, Bettinger et al. studied the internal rotation of allene[18] and found that the B3LYP internal rotational barrier was in a remarkably good agreement with coupled-cluster and multireference CI results. Bernardi et al.[19] investigated the cis−trans isomerization of small linear polyenes by means of DFT and CAS-PT2 methods. They also found a nice agreement between the corresponding B3LYP and CAS-PT2 rotational barriers.

The organization of the present paper is the following. The protonated and neutral Schiff bases are described separately because of significant differences between their electronic structures. Neutral Schiff bases do not take part in the dark adaptation process in BR. We discuss these species because they are important when one investigates changes in the proton affinity of imines during rotation around a double bond.[32] In both cases we start with the investigation of small model Schiff bases and verify the applicability of different quantum chemical methods for the description of the rotation around a double bond. In the protonated case a comparison of the experimental and theoretical vibrational spectra of a model Schiff base is also presented to help the verification of different theoretical methods. In the last part of each section larger Schiff bases are discussed including the complete *N*-methylretinal Schiff base structure.

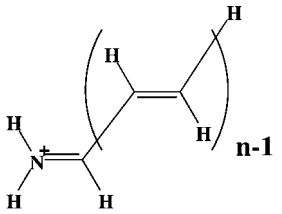

Figure 2. Schematic representation of the structure of the studied Schiff bases. The neutral or protonated imine group is conjugated to a polyacetylene chain of $n - 1$ units.

Computational Methods

For computer graphics and initial building of the molecular models we used Sybyl-6.3[20] running on a Silicon Graphics Indy workstation. Gradient optimization techniques were employed to optimize the geometries of the molecules at the RHF, UHF, DFT, CAS-SCF, and UNO-CAS levels of theory, using Pople's 6-31G(d) basis set. Except for the 90° rotated species, optimizations were performed without any geometry constraints. The hybrid Becke3LYP (Becke3, LYP) method was used for the DFT calculations. The calculations were performed with the GAUSSIAN-94[21] (RHF, UHF, CAS-SCF, DFT) and TX90[22] (UNO-CAS, UHF) program systems on an IBM SP2 machine.

The structure of the studied Schiff bases is schematically described in Figure 2. In each Schiff base (SB*n*) or protonated Schiff base (PSB*n*) structure, the terminal imine group is conjugated to a polyacetylene chain of $n - 1$ units. Regarding this analogy, the protonated and neutral species of unsubstituted Schiff bases can be described by $H_2N^+{=}CH(-CH{=}CH-)_{n-1}H$ and $HN{=}CH(-CH{=}CH-)_{n-1}H$, respectively. Atom numbering (N_1 to C_{12}) and bond numbering (B1 to B11) start from the nitrogen atom and its double bond, respectively, and continue toward the other end of the chain (Figure 1).

The initial guess orbitals for the CAS-SCF wave functions were selected from the π spaces of the investigated species. In the 90° rotated cases the molecules were rotated in space in order to place the "N1−C2−C3" part of the molecule into the *XY* plane and as much of the remaining part of the molecule as possible into the *YZ* plane. In the next step, the guess orbitals were carefully analyzed, and π orbitals were selected to be present in the active space (CAS). For example, in the case of the 90° rotated SB3 species we chose three orbitals with large π_z coefficients. These orbitals were mainly located on the N1, C2, and C3 atoms. After that, another three orbitals were selected with large π_x coefficients on the C4, C5, and C6 atoms. This procedure was carried out using the 6-31G basis, and the CAS-SCF/6-31G(d) calculations were started from the optimized CAS-SCF/6-31G wave function. In the unrestricted (UHF, UB3LYP) calculations the highest occupied (HOMO) and the lowest unoccupied (LUMO) molecular orbitals of the initial guess wave functions were mixed[23] (guess = mix keyword of Gaussian-94, USTA keyword of TX90). In many cases of the CAS-SCF and UNO-CAS calculations we have adopted Pulay's CAS selection rules.[24] Namely, the active space has been determined by those UHF natural orbitals (NO) that have significant fractional occupation (between 0.02 and 1.98). Also, in many cases, the UHF natural orbitals were used as initial guess orbitals for the CAS-SCF calculations.

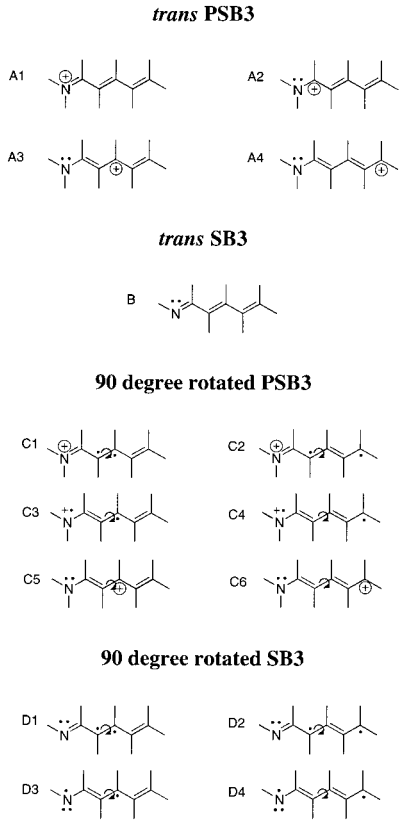

Figure 3. Mesomeric structures of the protonated and neutral SB3 species at the planar (trans) and 90° rotated arrangements of the atoms.

Results and Discussion

Protonated Schiff Bases. The mesomeric description of the *trans*-PSB3 molecule involves a few canonic forms (Figure 3). (The mesomeric structures are given only for the smallest PSB3 species; the corresponding forms can be easily derived for larger species.) The positive charge is carried by the N1, C2, C4, and C6 atoms in the A1, A2, A3, and A4 structures, respectively. The pattern of the double bonds varies in the mesomeric structures, indicating some bond length equalization along the chain. However, this effect decreases at the C terminal of the chain,[25,26] especially when longer chains are considered. The mesomeric structures belonging to the 90° rotated PSB3 species can be found in Figure 3. The first four structures (C1, C2, C3, and C4) are biradicaloids with the common characteristics that the positive charge is located on the N1 atom. The last two forms (C5 and C6) are free from any biradical character, and the positive charge is located on the "−C−C−C−" part of the molecule. These latter structures have some advantages over the biradical ones. In C5 and C6, the N1 atom is neutral, and the positive charge is carried by the C4 and C6 atoms, respectively. In the C5 and C6 structures, the "−C−C−C−" part of the molecule can be considered as an allyl cation-like species that is stabilized by delocalization of the π electrons. The weights of the closed-shell and biradical structures in the wave function are very important from the point of view of the applied quantum chemical model. As is well-known, rotation around a usual double bond cleaves the π-bond. This process can be considered as a particular case of bond dissociation that should be treated by using open-shell or multideterminant methods. On the other hand, the electronic structures dominated by closed-shell canonic forms could be described by a one-determinant-based methodology.

TABLE 1: Calculated Total Energies (hartree) and Rotational Barriers (kcal/mol) of Neutral and Protonated Schiff Bases

	trans	90° rotated	rotation barrier
	PSB3		
SCF	−248.198 734	−248.126 333	45.4
UHF	−248.200 277	−248.126 458	46.3
B3LYP	−249.828 684	−249.751 860	48.2
UB3LYP	−249.828 684[c]	−249.753 365	47.3[a]
CAS-SCF (2 × 2)		−248.147 870	61.0[b]
CAS-SCF (4 × 4)	−248.2450 90		
CAS-SCF (6 × 6)	−248.266 809	−248.178 535	55.4
	SB3		
SCF	−247.809 295	−247.648 464	100.9
UHF	−247.820 219	−247.782 750	23.5
B3LYP	−249.441 315	−249.329 186	70.4
UB3LYP	−249.441 315[c]	−249.367 416	46.4[a]
CAS-SCF (6 × 6)	−247.895 884	−247.814 207	51.3
UNO-CAS (6 × 6)	−247.893 267	−247.813 429	50.1
	PSB4		
SCF	−325.095 733	−325.040 141	34.9
UHF	−325.101 544	−325.042 245	37.2
B3LYP	−327.246 929	−327.184 848	39.0
UB3LYP	−327.246 929[c]	−327.184 870	38.9[a]
CAS-SCF (4 × 4)		−325.065 555	62.3[d]
CAS-SCF (6 × 6)	−325.164 907		
CAS-SCF (8 × 8)	−325.186 357	−325.117 525	43.2
	SB4		
SCF	−324.698 234	−324.545 566	95.8
UHF	−324.718 706	−324.684 305	21.6
B3LYP	−326.848 443	−326.744 362	65.3
UB3LYP	−326.848 443[c]	−326.781 488	42.0[a]
CAS-SCF (8 × 8)	−324.811 936	−324.736 580	47.3
UNO-CAS (8 × 8)	−324.808 783	−324.735 328	46.1
	PSB5		
B3LYP	−404.662 560	−404.609 645	33.2
	SB5		
UB3LYP	−404.255 896[c]	−404.192 903	39.5[a]
UNO-CAS (10 × 10)	−401.724 368	−401.654 448	43.9
	PSB6		
B3LYP	−482.076 444	−482.029 480	29.5
	SB6		
UB3LYP	−481.663 495[c]	−481.603 109	37.9[a]
UNO-CAS (12 × 12)	−478.639 992	−478.572 223	42.5
	N,4,8-trimethyl-PSB6		
B3LYP	−600.020 661	−599.979 178	26.0
	N,4,8-trimethyl-SB6		
UB3LYP	−599.607 073[c]	−599.550 380	35.6[a]
	Protonated *N*-Methylretinal Schiff Base		
B3LYP	−874.018 784	−873.981 387	23.5
	N-Methylretinal Schiff base		
UB3LYP	−873.596 511[c]	−873.539 694	35.7[a]

[a] The UB3LYP rotational barrier is calculated as the difference between the corresponding planar B3LYP and 90° rotated UB3LYP total energies. [b] The rotational barrier is calculated as the difference between the corresponding planar CAS-SCF (4 × 4) and 90° rotated CAS-SCF (2 × 2) total energies. [c] The UB3LYP solution collapsed to the closed-shell B3LYP one. [d] The rotational barrier is calculated as the difference between the corresponding planar CAS-SCF (6 × 6) and 90° rotated CAS-SCF (4 × 4) total energies.

The total energies and rotational barriers of the PSB3 molecule investigated by various methods can be found in Table 1. The "closed-shell type" RHF and B3LYP rotational barriers are close to each other (45.4 and 48.2 kcal/mol, respectively). In both the trans and 90° rotated cases an open-shell UHF solution was also found and the UHF rotational barrier (46.3 kcal/mol) is very close the RHF value (45.4 kcal/mol). While

TABLE 2: Comparison of Occupation Numbers of Natural Orbitals of Various Quantum Chemical Models[a]

method	π_1	π_2	π_3	π_4	π_5	π_6
			trans-PSB3			
UHF	1.997	1.972	1.839	0.161	0.028	0.003
CAS-SCF (4 × 4)	2.000	1.941	1.898	0.109	0.051	0.000
CAS-SCF (6 × 6)	1.960	1.935	1.893	0.116	0.059	0.037
			90° Rotated PSB3			
UHF	2.000	2.000	1.958	0.042	0.000	0.000
UB3LYP	1.999	1.998	1.821	0.179	0.002	0.001
CAS-SCF (2 × 2)	2.000	2.000	1.913	0.087	0.000	0.000
CAS-SCF (6 × 6)	1.998	1.935	1.911	0.072	0.067	0.017
			trans-SB3			
UHF	1.944	1.896	1.620	0.380	0.104	0.056
UNO-CAS (6 × 6)	1.937	1.912	1.855	0.152	0.086	0.057
CAS-SCF (6 × 6)	1.937	1.915	1.866	0.143	0.082	0.057
			90° Rotated SB3			
UHF	1.890	1.885	1.001	0.999	.115	0.110
UB3LYP	1.987	1.985	1.000	1.000	0.015	0.013
UNO-CAS (6 × 6)	1.900	1.898	1.001	1.000	0.102	0.099
CAS-SCF (6 × 6)	1.902	1.899	1.002	1.000	0.100	0.097

[a] The investigated systems are trans and 90° rotated PSB3 and SB3.

PSB3 at the trans arrangement of the atoms turned out to be triplet-stable at the B3LYP level of theory, we could find a lower energy open-shell UB3LYP solution at the 90° rotated species. The UB3LYP barrier (47.3 kcal/mol) calculated from the corresponding trans B3LYP and 90° rotated UB3LYP total energies is very close to the B3LYP (48.2 kcal/mol) value. The differences between the RHF and UHF total energies are small in the case of both trans and 90° rotated PSB3.

Analyzing the UHF natural orbitals (NOs) (Table 2), one can find that in the planar situation one π NO is nearly doubly occupied and that Pulay's CAS selection rules predict a "four electrons distributed to four orbitals" CAS. In the case of the 90° rotated species only two UHF NOs are partially occupied, indicating a 2 × 2 CAS description of the system. In both cases the energy lowering arising from the larger flexibility of the UHF wave function is small; therefore, the UHF rotational barrier is close to the RHF one. The UB3LYP NOs show similar behavior; one can find two orbitals with nonzero fractional occupancy at the 90° rotated case.

In Table 3 we present selected bond distances calculated at various levels of theory. As we mentioned above, the B3LYP method is triplet-stable at the planar arrangement of PSB3. However, we could find an open-shell UHF solution in this case. Comparing the respective closed-shell and UHF geometry parameters, one can find small differences only in the actual values of bonds B3, B4, and B5. In the case of the 90° rotated species the differences between the corresponding closed-shell and open-shell bond distances are very small for both the HF and DFT methods. These deviations at the UHF level are even smaller than the corresponding values at the planar situation.

The actual values of the rotational barriers computed at the HF and DFT levels of theory are close to each other and show a satisfactory performance of the investigated methods. (DFT is more preferable in this respect because the RHF method is subject to triplet instability at both the planar and 90° rotated arrangement of the atoms. On the other hand, DFT is triplet-unstable only at the 90° rotated geometry.) However, this is a very unusual situation, since polyenes are well-known for special effects that complicate their investigation by means of quantum chemical methods. These effects involve the problem of low-lying excited states at the planar arrangement and the strong biradical character of the transition structures of rotations around a double bond. Because many of these problems cannot be

TABLE 3: Comparison of Selected Bond Distances (angstrom) of Planar and 90° Rotated PSB3 and SB3 Species (for Abbreviations and Numbering, See Text)

method	B1	B2	B3	B4	B5
		trans-PSB3			
SCF	1.294	1.410	1.356	1.441	1.331
UHF	1.294	1.410	1.364	1.431	1.352
CAS-SCF (4 × 4)	1.287	1.424	1.359	1.450	1.347
B3LYP	1.315	1.407	1.375	1.431	1.352
CAS-SCF (6 × 6)	1.290	1.429	1.358	1.451	1.347
		90° rotated PSB3			
SCF	1.342	1.338	1.464	1.394	1.360
UHF	1.342	1.338	1.464	1.395	1.363
CAS-SCF (2 × 2)	1.342	1.338	1.464	1.400	1.365
B3LYP	1.347	1.363	1.452	1.403	1.373
UB3LYP	1.344	1.371	1.458	1.399	1.377
CAS-SCF (6 × 6)	1.360	1.347	1.468	1.394	1.369
		trans-SB3			
SCF	1.256	1.467	1.328	1.464	1.323
UHF	1.293	1.434	1.379	1.430	1.363
B3LYP	1.282	1.456	1.350	1.451	1.342
CAS-SCF (6 × 6)	1.280	1.473	1.345	1.466	1.324
UNO-CAS (6 × 6)	1.280	1.462	1.351	1.459	1.347
		90° rotated SB3			
SCF	1.281	1.408	1.423	1.434	1.339
UHF	1.319	1.403	1.478	1.397	1.389
B3LYP	1.306	1.420	1.442	1.409	1.369
UB3LYP	1.315	1.410	1.469	1.395	1.383
CAS-SCF (6 × 6)	1.308	1.413	1.480	1.393	1.390
UNO-CAS (6 × 6)	1.311	1.411	1.480	1.393	1.390

treated with methods based on one-determinant wave functions, we decided to investigate the electronic structure of the planar and 90° rotated PSB3 species by means of the CAS-SCF method. One of the most problematic point of a CAS-type method is the selection of the active orbitals. In many cases the selection is based on chemical intiution. For example, in CAS calculations of polyenes the number of active orbitals should be equal to the number of π centers ($\sigma-\pi$ separation). For more complicated situations one has to apply Pulay's CAS selection rules;[24] that is, the active orbitals should be selected on the basis of the fractionally occupied UHF natural orbitals. For those cases when the active orbitals can be selected on the basis of both techniques, the two active spaces should be the same. However, this is not the case for the investigated PSB3 species. Using Pulay's CAS selection rules, we have optimized the planar and the 90° rotated species at the CAS-SCF(4×4)/6-31G(d) and the CAS-SCF(2×2)/6-31G(d) levels of theory, respectively. The calculated CAS-SCF barrier is 61.0 kcal/mol, which is larger than the RHF, B3LYP, UHF, and UB3LYP barriers by 13−16 kcal/mol. On the other hand, as is the usual choice for investigating polyenes, we calculated total energies and barriers at the full 6 × 6 π space CAS-SCF level of theory. The calculated 6 × 6 CAS rotational barrier is 55.4 kcal/mol, still larger than those values corresponding to the RHF and DFT methods. This is a rather strange situation because in such a case when bond dissociation (π bond rotation) occurs, the closed-shell-type methods usually overestimate reaction barriers with respect to the experimental or CAS-SCF values. Investigating the occupational numbers of the CAS-SCF natural orbitals (Table 2), one can draw the following conclusions. At the planar arrangement of the atoms the "antibonding" NOs (π_4, π_5, π_6,) have small occupation numbers (0.116, 0.059, 0.037, respectively). However, the occupation numbers of the same orbitals at the 90° rotated geometry are even smaller, indicating that the electronic structure of this species is dominated by the closed-shell-type mesomeric structures. Comparing the optimized 6 × 6 CAS-SCF/6-31G(d) and (U)B3LYP/6-31G(d)

TABLE 4: Comparison of Occupation Numbers of Natural Orbitals of Various Quantum Chemical Models[a]

method	π_1	π_2	π_3	π_4	π_5	π_6	π_7	π_8
				trans-PSB4				
UHF	1.997	1.972	1.928	1.683	0.317	0.072	0.028	0.003
CAS-SCF (6 × 6)	2.000	1.947	1.926	1.882	0.131	0.069	0.046	0.000
CAS-SCF (8 × 8)	1.962	1.942	1.921	1.878	0.135	0.074	0.052	0.036
				90° Rotated PSB4				
UHF	2.000	1.999	1.970	1.809	0.191	0.030	0.001	0.000
UB3LYP	2.000	2.000	2.000	1.983	0.017	0.000	0.000	0.000
CAS-SCF (4 × 4)	2.000	2.000	2.000	1.925	0.059	0.017	0.000	0.000
CAS-SCF (8 × 8)	1.998	1.937	1.930	1.895	0.096	0.071	0.052	0.019
				trans-SB4				
UHF	1.944	1.921	1.839	1.497	0.503	0.161	0.079	0.056
UNO-CAS (8 × 8)	1.941	1.926	1.894	1.835	0.173	0.106	0.070	0.055
CAS-SCF (8 × 8)	1.941	1.927	1.901	1.851	0.159	0.099	0.068	0.054
				90° Rotated SB4				
UHF	1.929	1.887	1.824	1.001	0.999	0.176	0.113	0.071
UB3LYP	1.994	1.987	1.983	1.000	1.000	0.017	0.013	0.006
UNO-CAS (8 × 8)	1.925	1.899	1.872	1.002	1.001	0.130	0.100	0.072
CAS-SCF (8 × 8)	1.927	1.901	1.874	1.002	1.001	0.127	0.097	0.070

[a] The investigated systems are trans and 90° rotated PSB4 and SB4.

geometry parameters, one can find that at both the planar and 90° rotated species there exist some differences that are smaller for the rotated structure. The main difference between the CAS-SCF and B3LYP geometries is that the alternation of single and double bonds is more pronounced in the former case.

To further evaluate the performance of the investigated methods, we present total energies, rotational barriers, and selected occupational numbers of natural orbitals, as well as geometry parameters, for molecules PSB4 and SB4 in Tables 1, 4, and 5, respectively. Since the majority of the conclusions drawn from the PSB3 data is not affected by the elongation of the investigated polyene chain, we just briefly summarize the most important energetical and structural characteristics of PSB4.

The mesomeric description of the trans and 90° rotated PSB4 species is very similar to that of PSB3. The main difference between PSB3 and PSB4 is that in PSB4 the polyenyl unit is longer than the allyl cation-like C4−C5−C6 unit in PSB3. As a consequence, stabilization due to delocalization is more pronounced in the PSB4 case. This effect is very important in the case of the 90° rotated species where the positive charge is located on the polyenyl part of the molecules. Therefore, the PSB4 rotational barriers are smaller than the corresponding PSB3 values. Considering the energetics, the difference between the barriers predicted by the closed-shell-type RHF and B3LYP methods is larger in the case of PSB4 than in the PSB3 case. One has to note here that the RHF method shows triplet instability at both the planar and 90° rotated geometries, making the RHF description of the PES rather questionable. The UHF rotational barrier (37.2 kcal/mol) is closer to the B3LYP value (39.0 kcal/mol) than the RHF one (34.9 kcal/mol). While the B3LYP method is triplet-stable at the planar arrangement of the atoms, after many trials, we could find a lower-energy UB3LYP solution at the 90° rotated geometry. However, the energy lowering due to the larger flexibility of the UB3LYP model is smaller (0.014 kcal/mol) than the corresponding PSB3 value (0.9 kcal/mol). Furthermore, spin contamination present in the UB3LYP model is smaller for PSB4 (eigenvalue of the spin square operator ($\hat{S}^2$): 0.033) than the corresponding PSB3 value (eigenvalue of $\hat{S}^2$: 0.33).

Analyzing the occupational numbers of the UHF and UB3LYP natural orbitals, one can find similar tendencies observed in the PSB3 case. At the trans arrangement of the atoms one of the π UHF NOs is nearly doubly occupied, Pulay's CAS selection rules indicate a 6 × 6 CAS description of the system. At the 90° rotated case only four NOs remain fractionally occupied at the UHF level, indicating a 4 × 4 CAS wave function. At the UB3LYP level only two NOs are fractionally occupied and the occupancy of the π_5 NO is rather small (0.017, Table 4).

TABLE 5: Comparison of Selected Bond Distances (angstrom) of Planar and 90° Rotated PSB4 and SB4 Species (for Abbreviations and Numbering, See Text)

method	B1	B2	B3	B4	B5	B6	B7
				trans-PSB4			
SCF	1.301	1.397	1.368	1.421	1.350	1.448	1.329
UHF	1.299	1.403	1.373	1.413	1.378	1.426	1.362
B3LYP	1.323	1.398	1.385	1.412	1.374	1.433	1.351
CAS-SCF (6 × 6)	1.290	1.417	1.364	1.438	1.357	1.454	1.347
CAS-SCF (8 × 8)	1.293	1.423	1.362	1.439	1.357	1.454	1.347
				90° Rotated PSB4			
SCF	1.356	1.333	1.473	1.365	1.394	1.421	1.342
UHF	1.348	1.335	1.473	1.376	1.392	1.413	1.360
B3LYP	1.360	1.355	1.461	1.382	1.400	1.419	1.360
UB3LYP	1.359	1.356	1.461	1.382	1.401	1.419	1.360
CAS-SCF (4 × 4)	1.357	1.333	1.475	1.371	1.398	1.422	1.341
CAS-SCF (8 × 8)	1.371	1.345	1.475	1.374	1.395	1.422	1.357
				trans-SB4			
SCF	1.257	1.466	1.329	1.459	1.330	1.463	1.324
UHF	1.296	1.431	1.388	1.416	1.391	1.425	1.367
B3LYP	1.283	1.454	1.354	1.442	1.355	1.448	1.344
CAS-SCF (8 × 8)	1.278	1.463	1.351	1.457	1.352	1.460	1.346
UNO-CAS (8 × 8)	1.280	1.461	1.352	1.455	1.354	1.458	1.347
				90° Rotated SB4			
SCF	1.284	1.404	1.432	1.413	1.357	1.448	1.328
UHF	1.319	1.403	1.479	1.380	1.413	1.416	1.374
B3LYP	1.309	1.415	1.449	1.388	1.394	1.425	1.356
UB3LYP	1.316	1.409	1.471	1.373	1.411	1.416	1.364
CAS-SCF (8 × 8)	1.308	1.413	1.481	1.370	1.421	1.421	1.367
UNO-CAS (8 × 8)	1.311	1.410	1.482	1.371	1.420	1.420	1.368

Considering the geometry parameters (Table 5), the differences between the corresponding RHF and UHF values are larger at both the planar and 90° rotated arrangements of the atoms than was found for PSB3. On the other hand, the UB3LYP bond distances are very close to the B3LYP values. The barriers computed at the CAS-SCF level show similar tendencies found in the PSB3 case. The CAS-SCF rotational barrier using full π active spaces (8 × 8 CAS) for the whole PES is 43.2 kcal/mol. Using Pulay's CAS selection rules, we have optimized the planar and the 90° rotated species at the CAS-SCF(6×6)/6-31G(d) and the CAS-SCF(4×4)/6-31G(d)

TABLE 6: Comparison of Calculated Total Energies and Bond Distances and Theoretical and Experimental ν(C=N$^+$) and ν(C=C) Frequencies of $Me_2CHNH{=}CH{-}CH{=}CHMe^+$

	B3LYP/ 6-31G(d)	CAS−SCF/ 6-31G(d)	exptl[21, 22]
total energy (hartree)	−329.696 077	−327.511 441	
$R_{C=N}$ (Å)	1.302	1.284	
R_{C-C} (Å)	1.425	1.445	
$R_{C=C}$ (Å)	1.357	1.348	
ν(C=N$^+$) (cm^{-1})	1710	1862	1675
ν(C=C) (cm^{-1})	1681	1792	1638

levels of theory, respectively. The calculated CAS-SCF barrier is 62.3 kcal/mol, which is larger than the corresponding PSB3 value. Both CAS-SCF barriers are again larger than the RHF or DFT values. Considering the geometry parameters, the main difference between the CAS-SCF and B3LYP bond lengths is that the alternation of the CAS-SCF values is more pronounced than that of B3LYP.

Because of the deviations between the rotational barriers and geometry parameters predicted at the CAS-SCF and B3LYP levels, we decided to compare the theoretical results with experimental data. However, this is not an easy task in the case of protonated Schiff bases because the available experimental information is rather limited. Because of the lack of any crystallographic study on small protonated Schiff base salts, the available experimental data are restricted for FTIR results of small nonconjugated and conjugated imines.[27,28] In those studies Sándorfy and co-workers investigated various imine and acid mixtures in chloroform solution in order to understand the interaction of the retinal Schiff base with acidic amino acid side chains (glutamic and aspartic acids) in the protein environment. According to their results, the Schiff bases are protonated by the acids to some extent depending on the strength of the acid (both strong mineral and weaker organic acids were incorporated in their study) and on the particular Schiff base (conjugated or not). In the case of the protonated species, ion pairs are formed between the protonated base and ions derived from the acids. Back hydrogen bonds (like $N^+{-}H\cdots{}^-OOC$) play an important role in the stability of these structures. Sándorfy and co-workers did not assign all the peaks in the IR spectra; they paid attention to only those regions that were important from the point of view of Schiff base protonation. Fortunately, they assigned both the ν(C=N$^+$) and ν(C=C) peaks in the case of some small conjugated bases. So to further evaluate whether the B3LYP or CAS-SCF methods perform better in the case of small protonated conjugated imines, we carried out frequency calculations for one of the compounds investigated by Sándorfy and co-workers. One has to note in this respect that our calculations refer to gas-phase conditions while the experimental spectra were recorded in a chloroform solution where the electronic structure of the protonated Schiff base is perturbed by the negative ion of the ion pair. So perfect agreement is not expected from these comparisons. (Detailed investigation of these ion pair structures including the vibrational spectra is underway in our laboratory.) The particular molecular system used in the calculations is $Me_2CHNH{=}CH{-}CH{=}CHMe^+$, and the calculated total energies, selected bond distances, and theoretical and experimental ν(C=N$^+$) and ν(C=C) frequencies are shown in Table 6. In the CAS-SCF calculations we used a "four electrons distributed to four orbitals" CAS according to the size (two conjugated double bonds) of the system. The occupation numbers of the fractionally occupied UHF NOs were 1.985, 1.907, 0.093, and 0.015, respectively. Rigorous application of Pulay's CAS selection rules would indicate a 2×2 CAS wave function. However, the occupation numbers of orbitals π_1 and π_4 are very close to the threshold values of 1.98 and 0.02, respectively. Similar to those of the PSB3 and PSB4 molecules, the CAS-SCF bond distances show more pronounced alternation of the single and double bonds than that of the B3LYP method. This effect can be realized in the actual values of the ν(C=N$^+$) and ν(C=C) frequencies too because the CAS-SCF values are larger than the coresponding B3LYP ones by 152 and 112 cm^{-1}, respectively. The actual B3LYP/6-31G(d) ν(C=N$^+$) and ν(C=C) frequencies are rather close to the experimental values; the difference between the calculated and experimental frequencies are 35 and 42 cm^{-1}, respectively.

Therefore, one can conclude that the comparison of the experimental and theoretical frequencies further verify the use of the B3LYP/6-31G(d) method for the description of protonated Schiff bases. Taking into account also the theoretical considerations on the trans and 90° rotated PSB3 and PSB4 species described above, we can conclude that the B3LYP/6-31G(d) method presents a balanced description of the investigated double bond rotation and will be used for the study of larger species. In our opinion, the CAS-SCF method overestimates some antibonding interactions in the case of the PSB*n* molecules and it does not seem to be easy to set up a well-balanced CAS wave function for the whole PES.

In light of the comparisons described above, we should comment on the computational strategy applied by Logunov and Schulten in their recent work[14] on the dark adaptation process in BR. These authors carried out MD calculations based on classical force fields and used the CAS-SCF method for describing the chromophore at selected geometries. In the quantum chemical calculations the electrostatic effect of the protein environment was considered through explicit point charges in the electronic Hamiltonian. On the basis of our results, we can recommend the use of the B3LYP method for the in situ modeling of dark adaptation in a combined quantum chemistry and molecular dynamics (mechanics) study. The advantages of the B3LYP method are the following. Our calculations clearly proved that the B3LYP method provides us with a well-balanced description of a rotation of a double bond in protonated imines. The B3LYP method is numerically more stable than the CAS-SCF one; the large CAS-SCF runs are more expensive than the B3LYP ones. Therefore, the quantum chemical calculations could involve the whole *N*-methylretinal Schiff base (link atom approach) instead of Schulten's model compound, namely, 4-methyl-PSB6.

The B3LYP/6-31G(d) rotational barriers of the larger protonated Schiff bases are presented in Table 1. The mesomeric structures depicted in Figure 3 could be easily generalized for these cases and are not shown in order to save space. Similar to the PSB3 and PSB4 molecules, the *trans*-PSB*n* molecules exhibit some bond alternation that decreases close to the C terminal of the molecules. The electronic structure of the 90° rotated species can be considered as a competition between the closed-shell and biradical structures.

Concerning this competition, one has to mention that starting from PSB5 we could not find the UB3LYP solution at the 90° rotated species. This fact further confirms that the 90° rotated protonated species can be well described on the basis of the closed-shell-type B3LYP method. When the size of the investigated system is enlarged, the calculated rotational barriers gradually decrease to the value of 29.5 kcal/mol for PSB6. By investigating the last two structures, namely, *N*,4,8-trimethyl-PSB6 and the *N*-methylretinal Schiff base, we tried to model the rotation, which is important in the dark adaptation process of BR. Of course, these calculations do not involve special

electrostatic and steric effects of the protein environment, so this model should be considered as a first step toward the real description of the biological process. Such a question could be addressed by using hybrid quantum mechanics and molecular mechanics (QM/MM) methods[29−31] when the chromophore is described by quantum chemical methods and the protein environment is treated by classical force fields. (This work is in progress in our laboratory on the basis of our new ab initio QM/MM code.) The calculated rotational barriers of species *N*,4,8-trimethyl-PSB6 and the *N*-methylretinal Schiff base are 26.0 and 23.5 kcal/mol, respectively. These results can be understood by analyzing the generalized PSB6 version of the mesomeric structures depicted in Figure 3. At the planar situation the positive charge is carried by the N1, C2, C4, C6, C8, C10, and C12 atoms in the respective canonic forms. In both the *N*,4,8-trimethyl-PSB6 and the *N*-methylretinal Schiff base molecules, methyl groups are connected to the N1, C4, and C8 atoms. Furthermore, in the *N*-methylretinal Schiff base molecule the whole ionone ring is present with three additional methyl groups. The methyl groups have a large stabilizing effect on the positively charged molecule because of their hyperconjugation ability. For the 90° rotated species the electronic structure is dominated by the closed-shell-type structures depicted in Figure 3. In these structures the positive charge is carried by the C4, C6, C8, C10, and C12 carbon atoms, respectively. The carbon parts of these species can be considered as delocalized polyenyl cations. Since these structures are energetically not favorable, the hyperconjugation of the methyl groups stabilizing the 90° rotated structures is very important. In our opinion, behind the presence of delocalized π electron systems, the huge stabilizing effect of the methyl groups at the 90° rotated geometries can be responsible for such a small barrier like the actual 23.5 kcal/mol of the *N*-methylretinal Schiff base molecule.

Schiff Bases. In the case of the planar SB3 molecule the mesomeric description is dominated by the base structure of the molecule (B in Figure 3.). However, in the 90° rotated case, one can draw four biradical structures (Figure 3) from which the "−C−C−C−" part of the molecule can be assigned to an allyl radical like species.

The electronic structure of the planar SB*n* species is rather similar to the electronic structure of small polyenes (1,3,5-hexatrien in the case of SB3), so low-lying excited states can be important in the accurate description of the molecule. The closed-shell (RHF) wave function is triplet-unstable at both the planar and 90° rotated situations. Among the UHF NOs (Table 2) we have found nonzero fractional occupancies in the π space of the molecule, so a "six electrons distributed to six orbitals" CAS is predicted for both the planar and 90° rotated species by using Pulay's rules. It is worth mentioning that the planar and 90° rotated species are different from each other from the point of view of nondynamical correlation. In the case of the planar SB3, the nondynamical correlation is moderate and it originates from the presence of low-lying excited states. The 90° rotated SB3 molecule is a biradicaloid showing very strong nondynamical correlation effects.

The calculated SB3 rotational barriers vary over a wide range (Table 1). The RHF value (100.9 kcal/mol) is rather high; the rotation around a double bond can be considered as a particular case of bond dissociation that is unsatisfactorily described by the one-determinant RHF model. On the other hand, the UHF barrier is too small (23.5 kcal/mol), indicating some deficiencies in the UHF description of the planar structure. Examining the occupation numbers of the UHF NOs, one finds that the occupancies of the antibonding type π NOs (Table 2) are too large compared to the corresponding CAS-SCF or UNO-CAS values. Furthermore, the energy difference between the UHF and RHF total energies is rather small in the case of planar SB3, while the corresponding energy difference is large in the 90° rotated case. It is probable that the flexibility of the UHF wave function is small in the planar situation, so a multideterminant description of the system is mandatory.

The CAS-type methods (CAS-SCF, UNO-CAS) present a well-balanced description of the SB3 PES. The calculated CAS-SCF and UNO-CAS barriers, bond distances, and occupation numbers are very close to each other. The CAS-SCF (UNO-CAS) rotational barrier (51.3 and 50.1 kcal/mol) is reasonable in light of the RHF and UHF results.

Turning to the discussion of the DFT results, a rather interesting fact is that the B3LYP method is triplet-stable in the planar situation. It is another proof that the B3LYP model can describe not only dynamic but also moderate nondynamic correlation effects. Of course, in the 90° rotated case the B3LYP model becomes triplet-unstable, since the biradical structure cannot be described by a closed-shell model. The UB3LYP NOs (Table 2) show a clear biradical structure at the 90° rotated case. It is to be noted that the occupancies of the π_1 and π_2 NOs are closer to 2 than the occupancy of the corresponding orbitals in the CAS-SCF (UNO-CAS) case. Furthermore, the spin contamination in the case of the UB3LYP model is smaller than the UHF value. The UB3LYP rotational barrier calculated as the difference between the 90° rotated UB3LYP and the planar B3LYP total energies is not far from the corresponding CAS-SCF values.

The full set of calculations described above was carried out for the case of SB4, too. The SB4 results are presented in Tables 1, 4, and 5. The mesomeric description of the trans and 90° rotated SB4 species is very similar to that of SB3. The only difference is that stabilization due to delocalization is more pronounced in the SB4 case.

The RHF wave function is triplet-unstable again at both the planar and 90° rotated geometries. By use of Pulay's CAS selection rules,[24] an 8×8 CAS wave function is predicted for both the planar and 90° rotated species. In accordance with the SB3 data the RHF rotational barrier (95.8 kcal/mol) is too high and the corresponding UHF value (21.6 kcal/mol) is too low. The latter is probably due to the fact that the trans species is poorly described by the UHF method. (The occupation number of the π_5 NO is 0.503 at the UHF level.) On the other hand, the CAS-type methods present again a well-balanced description of the PES. The SB4 rotational barriers are 47.3 and 46.1 kcal/mol at the CAS-SCF(8×8)/6-31G(d) and UNO-CAS(8×8)/6-31G(d) levels of theory, respectively. The B3LYP model is triplet-stable at the planar arrangement of the atoms, while the UB3LYP NOs show a biradical structure at the 90° rotated case. The UB3LYP rotational barrier (42.0 kcal/mol) is reasonable compared to the CAS-SCF and UNO-CAS results.

In light of these results and because of the rather expensive nature of the CAS-SCF method, further calculations on the rotational barrier of the SB*n* Schiff bases have been restricted to the use of UNO-CAS and UB3LYP methods. Generally, the UNO-CAS and UB3LYP rotational barriers are close to each other. In agreement with chemical intuition, both methods predict decreasing barriers when the investigated systems are enlarged.

In the case of the largest systems we have calculated the rotational barriers only at the UB3LYP level of theory. The rotational barriers of *N*,4,8-trimethyl-SB6 (35.6 kcal/mol) and

the *N*-methylretinal Schiff base (35.7 kcal/mol) are close to the SB6 value (37.9 kcal/mol), indicating that the most important stabilization effects arise from the delocalized π electron structure. The chain atoms of the unprotonated Schiff base molecules are nearly neutral, so the stabilization effect of the methyl groups on the charged parts of the molecules is not significant.

Acknowledgment. We thank Professor I. Mayer for valuable discussions on the problem of bond alternation.

References and Notes

(1) Spudich, J. L.; Bogomolni, R. A. *Annu. Rev. Biophys. Biophys. Chem.* **1988**, *17*, 193.
(2) Henderson, R.; Baldwin, J. M.; Ceska, T. A.; Zemlin, F.; Beckmann, E.; Downing, K. H. *J. Mol. Biol.* **1990**, *213*, 899.
(3) Trissl, H. W. *Photochem. Photobiol.* **1990**, *51*, 793.
(4) Mathies, R. A.; Lin, S. W.; Ames, J. B.; Pollard, W. T. *Annu. Rev. Biophys. Biophys. Chem.* **1991**, *20*, 491.
(5) Oesterhelt, D.; Tittor, J.; Bamberg, E. *J. Bioenerg. Biomembr.* **1992**, *24*, 181.
(6) Rotschild, K. J. *J. Bioenerg. Biomembr.* **1992**, *24*, 147.
(7) Lanyi, J. K. *J. Bioenerg. Biomembr.* **1992**, *24*, 169.
(8) Khorana, H. G. *Proc. Natl. Acad. Sci. U.S.A.* **1993**, *90*, 1166.
(9) Ebrey, T. G. In *Thermodynamics of membrane receptors and channels*; Jackson, M. B., Ed.; CRC Press: Boca Raton, FL, 1993; pp 353−387.
(10) Lanyi, J. K. *Biochim. Biophys. Acta* **1993**, *1183*, 241.
(11) Krebs, M. P.; Khorana, H. J. *J. Bacteriol.* **1993**, *175*, 1555.
(12) Mukohata, Y.; Ihara, K. K.; Uegaki, Y. M.; Sugiyama, Y. J. *Photochem. Photobiol.* **1991**, *54*, 1039.
(13) Warshel, A. *Nature* **1976**, *260*, 679.
(14) Logunov, I.; Schulten, K. *J. Am. Chem. Soc.* **1996**, *118*, 9727.
(15) Roos, B. O. *Adv. Chem. Phys.* **1987**, *69*, 399 and references therein.
(16) Bofill, J. M.; Pulay, P. *J. Chem. Phys.* **1989**, *90*, 3637.
(17) Kozlowski, P. M.; Rauhut, G.; Pulay, P. *J. Chem. Phys.* **1995**, *103*, 5650.
(18) Bettinger, H. F.; Schreiner, P. R.; Schleyer, P. v R.; Shaefer, H. F., III. *J. Phys. Chem.* **1995**, *100*, 16147.
(19) Bernardi, F.; Garavelli, M.; Olivucci, M.; Robb, M. A. *Mol. Phys.* **1997**, *92*, 359.
(20) TRIPOS Associates, Inc.
(21) Frisch, M. J.; Trucks, G. W.; Schlegel, H. B.; Gill, P. M. W.; Johnson, B. G.; Robb, M. A.; Cheeseman, J. R.; Keith, T.; Petersson, G. A.; Montgomery, J. A.; Raghavachari, K.; Al-Laham, M. A.; Zakrzewski, V. G.; Ortiz, J. V.; Foresman, J. B.; Cioslowski, J.; Stefanov, B. B.; Nanayakkara, A.; Challacombe, M.; Peng, C. Y.; Ayala, P. Y.; Chen, W.; Wong, M. W.; Andres, J. L.; Replogle, E. S.; Gomperts, R.; Martin, R. L.; Fox, D. J.; Binkley, J. S.; Defrees, D. J.; Baker, J.; Stewart, J. P.; Head-Gordon, M.; Gonzalez, C.; Pople, J. A. *Gaussian 94*, revision C.3; Gaussian, Inc.: Pittsburgh, PA, 1995.
(22) Pulay, P. TX90, Fayetteville, AR 1990. (b) Pulay, P. *Theor. Chim. Acta* **1979**, *50*, 229.
(23) Pulay, P.; Liu, R. *J. Phys. Chem.* **1990**, *94*, 5548.
(24) Pulay, P.; Hamilton, T. P. *J. Chem. Phys.* **1988**, *88*, 4926.
(25) Tajkhorshid, E.; Paizs, B.; Suhai, S. *J. Phys. Chem. B* **1997**, *101*, 8021.
(26) Froese, R. D. J.; Komáromi, I.; Byun, K. S.; Morokuma, K. *Chem. Phys. Lett.* **1997**, *272*, 335.
(27) Lussier, L. S.; Dion, A.; Sándorfy, C.; LeThanh, H.; Vocelle, D. *Photochem. Photobiol.* **1986**, *44*, 629.
(28) Lussier, L. S.; Sándorfy, C.; LeThanh, H.; Vocelle, D. *Photochem. Photobiol.* **1987**, *45*, 801.
(29) Warshel, A.; Lewitt, M. *J. Mol. Biol.* **1976**, *103*, 227.
(30) Field, M. J.; Bash, P. A.; Karplus, M. *J. Comput. Chem.* **1990**, *11*, 700.
(31) Bakowies, D.; Thiel, W. *J. Phys. Chem.* **1996**, *100*, 10580.
(32) Tajkhorshid, E.; Paizs, B.; Suhai, S. *J. Phys. Chem.*, submitted for publication.